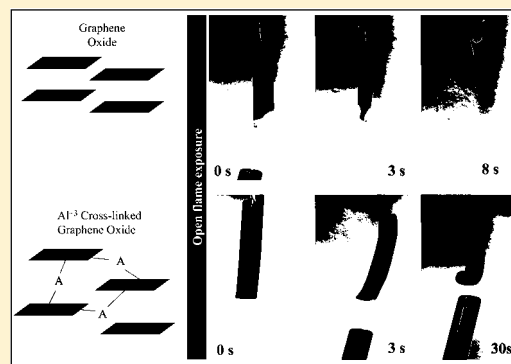


# Multivalent Cation Cross-Linking Suppresses Highly Energetic Graphene Oxide's Flammability

Hulusi Turgut,<sup>†,‡</sup> Z. Ryan Tian,<sup>\*,†,‡,§</sup> Fengjiao Yu,<sup>||</sup> and Wuzong Zhou<sup>||</sup><sup>†</sup>Microelectronics/Photonics, <sup>‡</sup>Institute of Nanoscience/Engineering, and <sup>§</sup>Chemistry/Biochemistry, University of Arkansas, Fayetteville, Arkansas 72701, United States<sup>||</sup>School of Chemistry, University of St Andrews, St Andrews KY16 9ST, U.K.

## Supporting Information

**ABSTRACT:** Graphene oxide (GO), a common intermediate for making graphene-like materials from graphite, was recently found to possess an explosive fire hazard that can jeopardize the GO's large-scale production and wide applications. This work reports a simple and facile method to cross-link the GO with Al<sup>3+</sup> cations, in one step, into a freestanding flexible membrane. This inorganic membrane resists in-air burning on an open flame, at which non-cross-linked GO was burnt out within ~5 s. All characterization data suggested that the in situ "epoxy ring-opening" reactions on the GO surface facilitated the cross-linking, which elucidated a new mechanism for the generalized inorganic polymerization. With the much improved thermal and water stabilities, the cross-linked GO film can help to advance high-temperature fuel cells, electronic packaging, etc. as one of the long-sought inorganic polymers known to date.



## INTRODUCTION

Recently, graphene-based new materials have attracted enormous excitement, thanks to their excellent mechanical and electrical properties on top of their highly accessible specific surface area. In the search for better and cheaper routes to synthesizing these materials,<sup>1–7</sup> chemical modification of graphene oxide (GO) is considered the most easily scalable to date.<sup>8–16</sup> This is because, sterically, the modification can easily take place on the oxygenated functional groups (e.g., >O, –OH, –COOH, etc.) that form mostly on the GO edge for exfoliating graphite layers and dispersing GOs in aqueous and organic solvents. On the GO surface, the energetic epoxide group was recently found to make the GO highly flammable,<sup>17</sup> and inorganic byproducts including potassium and sodium salts (i.e., the residue from the GO synthesis) were shown to contribute significantly to the violent combustibility of the GO in ambient air. This fire hazard causes the GO to be a dangerous material,<sup>18–21</sup> especially for the partially reduced GO (or rGO). Hence, a new method should be developed timely for facilely mass producing flame-retardant and highly thermal-stable GO.<sup>22</sup>

Herein, we report a new and simple method for mass producing such nonflammable GO, by cross-linking the GO with Al<sup>3+</sup> cations in one step in aqueous solutions at room temperature. The cross-linked GO (cl-GO) resists combustion in ambient air on open flame and shows in addition a greatly improved thermal stability, which ended the above-mentioned fire hazard. This thermally stable cl-GO can be applicable to making devices operational at elevated temperatures (above 120 °C) even in air, such as high-temperature fuel cells, high-

temperature coating, and thermally stable electronic packaging, to name a few. Our characterization data further suggest that the cross-linked GO inherited all characteristics of ordinary GO except the flammability, and its good dispersibility in water is widely fine-tunable, which greatly expands the new cl-GO's processability and in turn its wide applicability on an industry scale.

## EXPERIMENTAL METHODS

**Chemical Synthesis of GO.** The GO was prepared by mixing 0.5 g of graphite powder (Alfa Aesar, natural, briquetting grade, -200 mesh, 99.9995% metal basis) and 0.5 g of NaNO<sub>3</sub> (Alfa Aesar, 98+%) into 23 mL of concentrated H<sub>2</sub>SO<sub>4</sub> (BDH Aristar, 95–98% min) solution, under stirring in an ice bath for 15 min. This was followed by adding 4 g of KMnO<sub>4</sub> (J.T. Baker, 99% min) gradually under stirring for another 30 min in an ice bath and then transferred into a 40 °C water bath under a stirring for about 90 min. The resultant paste was diluted by 50 mL of deionized water, then stirred for 15 min, and then mixed with 6 mL of H<sub>2</sub>O<sub>2</sub> (Alfa Aesar 29–32% w/w) and 50 mL of distilled/deionized (DDI) water. The resultant product was washed with a copious amount of DDI water and dried at 40 °C in air over 24 h.

**Synthesis of Aluminum Cross-Linked Graphene Oxide (cl-GO).** An amount of 300 mg of GO was dispersed in 100 mL of DDI water under agitation. Separately, 0.2 g of Al(NO<sub>3</sub>)<sub>3</sub>·

Received: December 28, 2016

Revised: February 13, 2017

Published: February 21, 2017

9H<sub>2</sub>O (EM Science) was added to another 100 mL flask pre-filled with DDI water. The GO dispersion was gradually added into the aluminum nitrate solution, and the resultant cl-GO was stirred for 5 min at room temperature, then washed with a copious amount of DDI water for several times.

**Fabrication of GO and cl-GO Films.** The same amounts of dispersed cl-GO and GO (1 mg/mL) were used to fabricate films on various substrates such as silicon wafer, polystyrene, polyethylene terephthalate, polytetrafluoroethylene, glass slide, and plastic paraffin film. The best defect-free and durable freestanding GO and cl-GO films were formed on polystyrene substrates using drop-casting methods. Thus, cast films were dried in air over 24 h at room temperature.

**Characterizations.** The GO and cl-GO samples were analyzed by means of a PHI Versa probe scanning X-ray photoelectron spectroscopy (XPS) microprobe equipped with dual-beam charge neutralization and a monochromatic Al K $\alpha$  source (1486 eV). Surveys were obtained with a 117 eV pass energy and 1.0 eV step size, while high-resolution spectra were obtained with 23.5 eV pass energy with 0.1–0.2 eV step size and with the time of 25 ms per step. For charge correction, 284.8 eV was used as the adventitious carbon peak position, and peak positions were determined by the curve-fitting method.

Thermogravimetric analysis (TGA) tests were performed on TGA Q50 V20.10 Build 36 under N<sub>2</sub> flow, with the samples being heated from room temperature to 350 °C at the ramping speed of 15 °C/min. The differential scanning calorimetry (DSC) results were obtained in a N<sub>2</sub> flow (20 mL/min) on a PerkinElmer Pyris Diamond differential scanning calorimeter for 5 mg of each sample, first being heated at 50 °C for 1 min then heated to 300 °C at a speed of 10 °C/min. The X-ray powder diffraction (XRD) patterns were obtained from a Rigaku MiniFlex II Desktop XRD using monochromatized Cu K $\alpha$  radiation ( $\lambda = 1.5418 \text{ \AA}$ ) at 30 kV and 15 mA, in the range of 2-theta from 5° to 60° at a speed of 0.1°/min. High-resolution scanning electron microscopy (SEM) images were obtained using a FEI Nova Nanolab 200 Duo-Beam Workstation being operated on a 15 kV electron beam. An in-house built Raman spectroscope equipped with 532 nm laser source at 3 mW was used to obtain the microRaman spectra. For estimating surface area using the methylene blue absorption method, the known masses of GO and cl-GO were separately soaked into an aqueous solution of methylene blue in 25 mL flasks and then stirred at 400 rpm for 48 h. Then the samples were centrifuged, and the supernatant's concentration was analyzed using ultraviolet visible spectroscopy (wavelength of 661 nm, U-0080D) for comparison against the original concentration and knowing the methylene blue molecules being adsorbed. Transmission electron microscopy (TEM) images were obtained on a JEOL-2011 electron microscope operating at 200 kV equipped with an Oxford Link ISIS system for energy-dispersive X-ray spectroscopy (EDX).

## RESULTS/DISCUSSION

It was detailed in the literature that even an air-drying temperature near 100 °C can trigger a thermal reduction–decomposition of GO, which is potentially dangerous in large-scale manufacturing.<sup>17</sup> This is because such a decomposition of GO is as highly exothermic as almost self-igniting that must be absolutely avoided in any large-scale manufacturing. Moreover, it was indicated in the literature that residual potassium salts, from the GO synthesis involving KMnO<sub>4</sub> or K<sub>2</sub>S<sub>2</sub>O<sub>8</sub>, can

readily transform to various potassium-containing impurities<sup>18</sup> that can turn the GO to the extremely flammable forms. Removing these impurities via filtration or dialysis is time consuming and costly because GO flakes easily clog the filter pores and reduced the water flow across the filtering media (e.g., anodized aluminum oxide or AAO). Washing with abundant water was proven troublesome in our experiment because after a few washing cycles the GO started to increasingly gelatinize which drastically increased the time and manpower in the follow-up centrifugal separations. Further, both the filtration and washing still resulted in the GO flakes with energetic epoxide groups that can cause the GO to be flammable.<sup>17</sup> Thus, an increasing concern has been seriously raised about the fire hazard of the GO in especially its large-scale production and applications.<sup>19–21</sup>

Our experiment started from the GO synthesis (Figure 1a) using a modified Hummer's method,<sup>22</sup> and the resultant GO

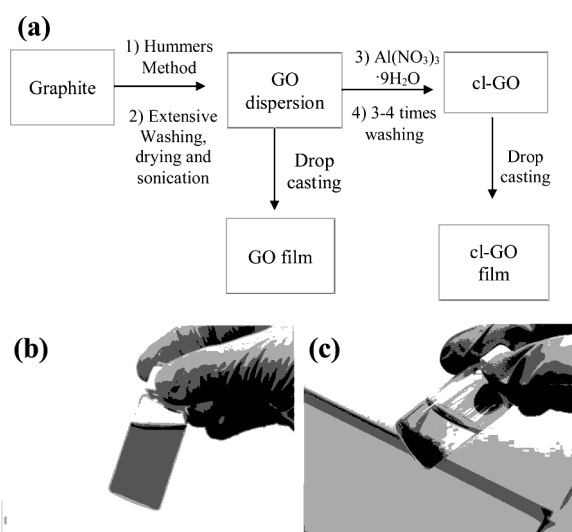


**Figure 1.** (a) Flowchart for fabricating the GO and cl-GO. (b) A GO solution (0.5 mg/mL); (c) 1 min after the GO being cross-linked in the aqueous solution (1.0 wt %) of Al(NO<sub>3</sub>)<sub>3</sub>.

was washed with water and centrifugation. The GO material was then dried in an oven and thereafter exfoliated in DDI water using ultrasonication. The suspension of the exfoliated GO was added into an aqueous solution (1.0% w/w) of Al(NO<sub>3</sub>)<sub>3</sub> under vigorous stirring, in order for the cross-linking to take place instantly at room temperature (Figure 1b,c). This cross-linking was followed by a few times of washing with DDI water, for further reducing the K-containing impurities' content. Afterward, 100 mL of the GO suspension was centrifuged at 4000 rpm for an hour, and the resultant GO precipitate was collected and then drop-cast on a glass-slide surface to dry into a thin flexible freestanding membrane about 15–20  $\mu\text{m}$  thick. The cl-GO membrane, together with another similar-sized GO film but without the cross-linking, were each exposed to an open flame from a commercial lighter (burning the butane fuel) in air.

In chemical science, the alkaline earth metal cation is a fairly strong Lewis acid that can form a strong bond on GO, by inducing a ring-opening reaction<sup>1</sup> of the epoxide (a Lewis base) on the GO. The epoxide groups are mainly accountable for the energetic behavior of GO, and hence the ring-opening reaction on the epoxide group can alter the thermal decomposition

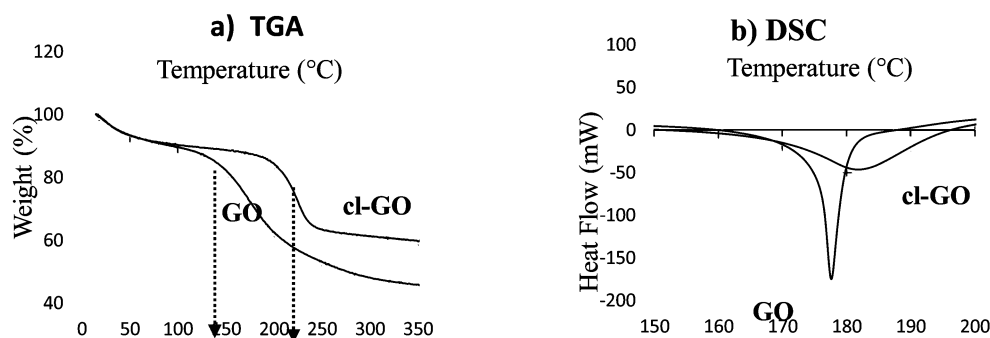


**Figure 2.** (a) TGA curves of GO and cl-GO, from a heating at 15 °C/min under a N<sub>2</sub> flow, showing the mass loss for cl-GO near 200 °C and that for GO near 125 °C. (b) DSC curves of GO and cl-GO, from a heating at 10 °C/min under a N<sub>2</sub> flow, showing the heat release (the exothermic peak) of the energetic GO being much greater than that of the thermally stable cl-GO.

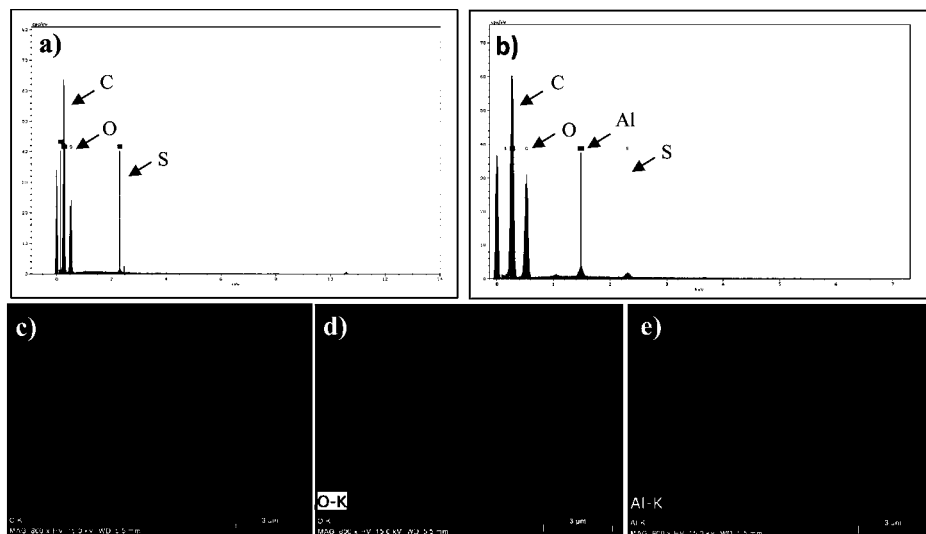


**Figure 3.** Elemental analysis results from (a) GO and (b) cl-GO and the supporting elemental mapping of (c) carbon, (d) oxygen, and (e) aluminum.

kinetics.<sup>17</sup> This motivated us to propose logically and prove in experiment whether this concept's applicability could be expanded to using trivalent metal cations such as Al<sup>3+</sup> (a much stronger Lewis acid) to bond with oxygen-containing functional groups including epoxide and carboxylic acid groups in between two adjacent GO sheets, in either a face-to-face or a shoulder-by-shoulder manner or even both.

Combustion rapidly propagating caused the GO film to vanish (or gasify) in ~5 s, while no combustion (besides reduction) took place on the cl-GO film even after a minute (see videos in the [Supporting Information](#)). Since the open flame is an easily accessible heat source for GO reduction in scale-up production, we were motivated to further investigate the thermal behavior of the GO film and the cl-GO film.

Thermogravimetric analysis (TGA) data of GO and cl-GO were compared in [Figure 2a](#). A minor mass loss for both samples at 100 °C can be attributed to the desorption of physisorbed water on the samples, while the major mass losses at 100–300 °C are due to the pyrolysis of the oxygen-containing functional groups. The cl-GO exhibited a slower mass loss starting around 200 °C, while that of the GO appeared at 125 °C in a faster rate.

Differential scanning calorimetry (DSC) results ([Figure 2b](#)) further suggested that the GO's thermal decomposition process is much more exothermic than the cl-GO's. Intuitively, the

excessive and abrupt heat release of GO from the deoxygenation reaction can trigger the combustion. In contrast, the heat effect of the cl-GO was much smaller. The DSC data, together with the TGA's, proved the Al<sup>3+</sup>-cross-linked GO polymer's thermal-stable nature, which prompted us to further characterize the GO's and cl-GO's other structural and surface properties.

In thermochemistry, GO's decomposition can shift to the more exothermic site due to an increased content of epoxide and to the more endothermic due to an increased hydroxyl content.<sup>17</sup> The TGA-DSC data suggest that cross-linking Al<sup>3+</sup> cations on every GO sheet triggered the epoxide ring-opening reaction which decreased the epoxide group's content and in turn increased the hydroxyl group content on cl-GO.

For further verifying potassium and sulfur salts' role in the flammability of GO,<sup>21</sup> a GO film and a cl-GO film were soaked into a 1.0 wt % aqueous solution of KOH for 5 min and then dried and open-flamed. Again, the GO film was ignited instantly and disappeared quickly, while cl-GO film was not combusted. This study further concluded the cl-GO film's nonflammable nature.

An elemental analysis revealed that GO and cl-GO films have sulfur content of 0.17 at. % and 0.21 at. %, respectively, even after being washed extensively with DI water under centrifugation ([Figure 3](#)). Surprisingly, as little as 0.42 at %

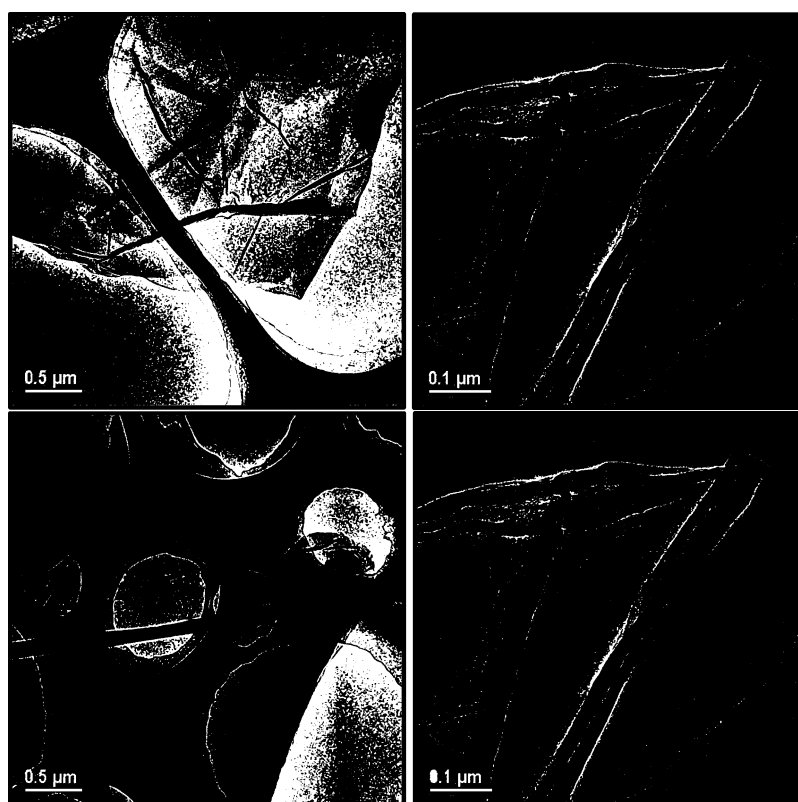


**Figure 4.** TEM image of cl-GO. (a) Characteristic wrinkled GO sheet. (b) and (c) Few layers of overlapped and cross-linked GO sheets. (d) High-resolution image of the cl-GO sheets.

aluminum has led to the GO polymerization into the cl-GO within a few seconds. Elemental analysis mapping results of cl-GO also showed that Al sparsely distributed along the flakes.

The transmission electron microscopic (TEM) image in Figure 4a disclosed the wrinkled nature of graphene sheets. Figure 4b,c further shows that the cl-GO sheets are linked up on the GO edges, and the split ends of two adjacent sheets can be seen in Figure 4c. Under a higher magnification (Figure 4d), a darker middle section is probably due to the existence of a higher content of Al elements.

New reports in the literature have indicated that epoxide groups of GO are mainly responsible for GO's high flammability, and alteration of these groups can minimize the energetics.<sup>17,18,21</sup> Thus, we proposed that reducing epoxide groups or all oxygenated functional groups of GO may further minimize the fire hazard. However, it was argued that even the reduced GO (called rGO) can still be extremely flammable due to the residue byproducts from the synthesis process of GO.<sup>18</sup> On the other hand, the applications can be limited if all oxygenated functional groups are removed in GO. Thus, cl-GO possesses unique advantages, by eliminating high flammability of GO without disturbing a major portion of oxygenated groups. The flame resistance and retardancy of cl-GO can be explained by the two major mechanisms: (i) partial pacification of epoxide groups via cross-linking them with Al<sup>3+</sup> cations and (ii) shielding heat propagation between the GO flakes to result in the cl-GO with superior thermal stability and open flame resistance. One such study reported that upon heating GO the heat transferred from one highly energetic GO site to another very rapidly,<sup>18</sup> which matches our results from this work. Our DSC results suggested that when once GO was heated a thermal decomposition started to propagate quickly with rapid

heat accumulation which is in line with other reports on the same phenomena. However, when cl-GO was heated, much less heat accumulation between GO flakes prevented the excessive heat accumulation that results in a serious fire hazard.

Surprisingly, some studies in the literature claimed that GO and its derivatives can be used as a potential flame-retardant polymer additive despite its highly energetic structure and thermal instability.<sup>23–29</sup> In contrary, a recent review on GO's thermal instability seriously questioned its use for flame-retardant applications and pointed out that GO or contaminated rGO may behave like a fuel for combustion rather than a flame-retardant additive material.<sup>21</sup> The results in the review suggest that there is a strong association between the number of epoxide groups, the amount of synthesis byproducts, and GO's flammability. For timely clarifying of the confusion in the literature, our cl-GO can be a very strong candidate to resolve the above-mentioned issues with its thermal stability and flame-resistant properties.

Freestanding flexible films made of GO were demonstrated to be highly promising in many important applications in solutions,<sup>30–35</sup> owing to their unique properties such as high tensile strength, proton conductivity, and durability in water. In the literature,<sup>36–40</sup> however, negatively charged GO was found to be soluble in water owing to the presence of the residual metal cations, and Al<sup>3+</sup> on the anodized aluminum oxide filter was reported to improve the GO sheets mechanical strength.<sup>40</sup> Hence, in our experiment by sonicating a GO film and a cl-GO film in water for 10 min the GO film became fragmented, while the cl-GO film remained intact, which defined a need to study the cl-GO's unusual microstructure.

The cross-linking was further supported by the Fourier-transform infrared (FT-IR) spectra (Figure 5a). In comparison

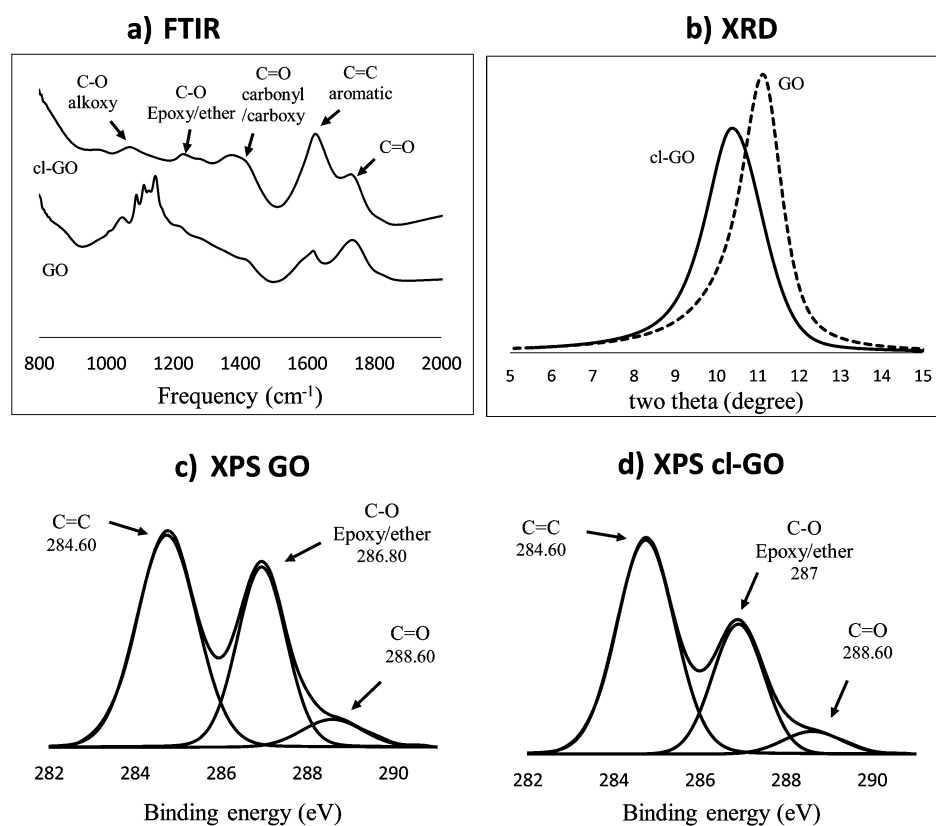


**Figure 5.** Characterizations of GO and cl-GO. (a) FT-IR spectra; (b) XRD patterns; (c) deconvoluted XPS spectra of GO; and (d) cl-GO.

with the GO's typical vibrations for C=O ( $1733\text{ cm}^{-1}$ ), aromatic C=C ( $1618\text{ cm}^{-1}$ ), carbonyl (or carboxyl) C–O ( $1411\text{ cm}^{-1}$ ), epoxy C–O ( $1226\text{ cm}^{-1}$ ), and alkoxy C–O ( $1057\text{--}1149\text{ cm}^{-1}$ ), the cl-GO showed a much lower C=O intensity. This suggests that the GO's energetic epoxy groups were reacted with the  $\text{Al}^{3+}$  cations through the ring-opening reaction, which decreased the content and hence intensity of the epoxy vibration. Moreover, the vibration was slightly “red”-shifted to a lower frequency probably because of the leftover ether-like functional groups that are hard to react with the Al(III) cations.

In powder X-ray diffraction (XRD) data (Figure 5b), the main diffraction peak of the GO sample appears at 2-theta of  $11.4^\circ$  (a lower d-space) and that of cl-GO at  $10.39^\circ$  (a higher d-space). This difference proves that upon cross-linking the d-space in between the stacked cl-GO flakes was increased by the “sandwiched”  $\text{Al}^{3+}$  cations, from 0.79 nm in GO to 0.85 nm in cl-GO. The thus-increased interlayer spacing is a strong evidence of the intercalating cross-linking of the Al(III) cations in between the cl-GO flakes.

The epoxide ring opening of GO polymerization is suggested by X-ray photoelectron spectroscopy (XPS) data of C 1s signals of the GO and cl-GO samples (Figure 5c,d). The C–O peak is mainly due to the epoxy/ether groups, and the C=O peak is due to the carboxyl and ketone groups. The C–C, C–O, and C=O peaks for GO ought to appear at 284.6, 286.8, and 288.56 eV, respectively. The C–C, C–O, and C=O peaks for cl-GO, however, were instead recorded at 284.6, 287.0, and 288.6 eV, respectively. On a much lower intensity, the C–O signal (epoxy/ether peak) of cl-GO significantly shifted upward by 0.2 eV (i.e., more stable or less energetic), which is in line with the epoxide-ring-opening reaction with Al(III) cations.

The micro-Raman spectra of GO exhibit two broad peaks at  $1593$  and  $1355\text{ cm}^{-1}$  corresponding to the G and D bands, respectively (Figure 6). The G peak is associated with the first-

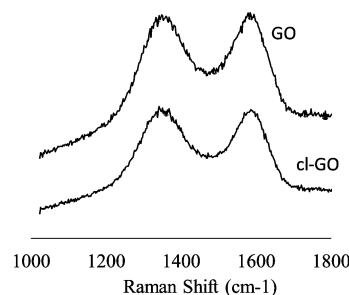


**Figure 6.** Micro-Raman spectra of GO and cl-GO.

order  $E_{2G}$  mode, while the D peak is associated with disordered structure of graphite.<sup>41,42</sup> It has been consistently reported that removing oxygenated functional groups from GO can result in an increased D/G signal-intensity ratio because of the defects from the reduction.<sup>43</sup> Further, the increased D/G signal-intensity ratio has been consistently observed upon reduction of GO, which could be attributed to the enhanced graphitic structure of GO.<sup>41–46</sup> Accordingly, in this study, the cross-linking changed the D/G signal-intensity ratio, from 1.06 in GO to 1.11 in cl-GO. This slight increase in the D/G signal-intensity ratio of cl-GO suggests that the graphitic character was slightly increased in the cl-GO upon the cross-linking process.

In the literature,<sup>47</sup> the methylene blue adsorption method is recommended as a simple and effective method to estimate graphitic material's surface area, in which each adsorbed

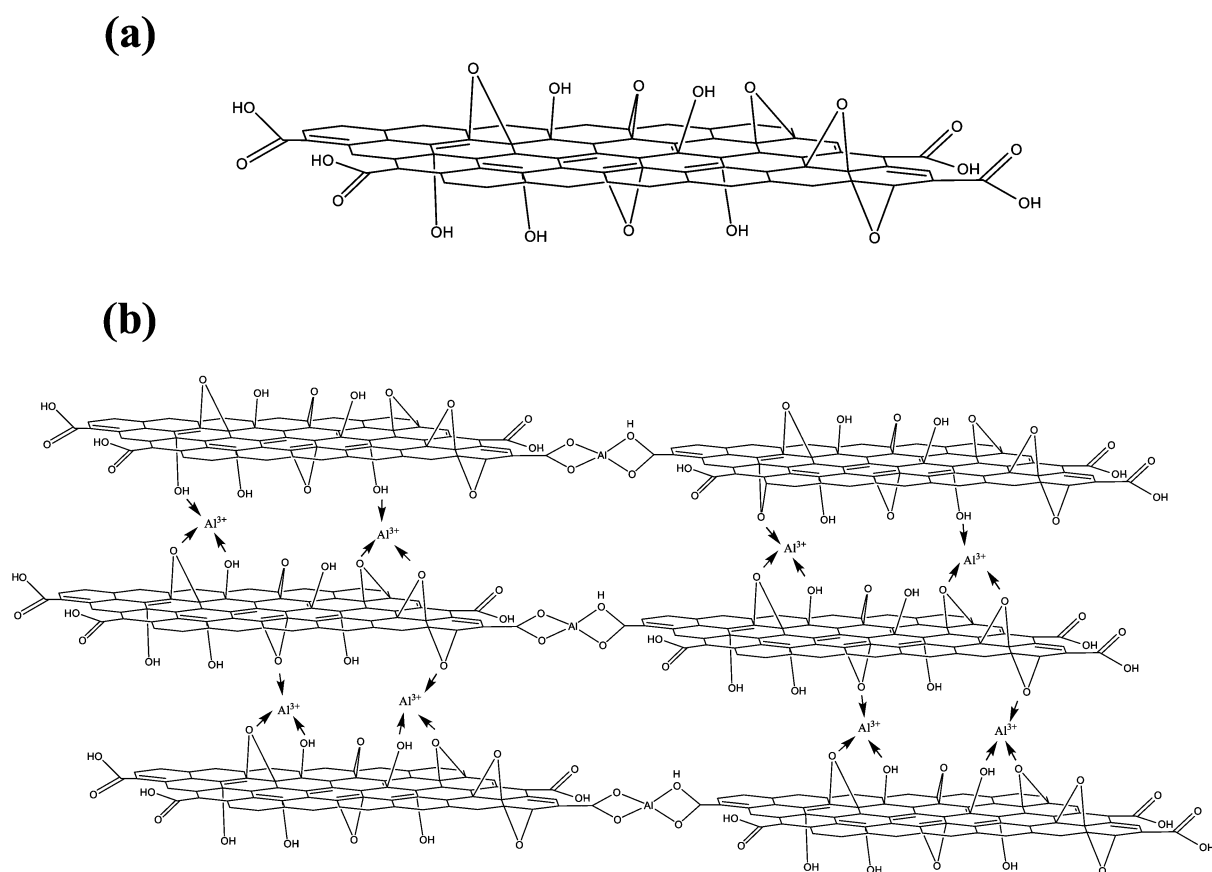


**Figure 7.** Illustration of cl-GO polymer's microstructure. (a) GO and (b) cl-GO.

methylene blue's cross-sectional surface area is about 1.35 nm<sup>2</sup>. We, using this method, estimated the surface area of GO and cl-GO to be 645 and 735 m<sup>2</sup>/g, respectively. The extra 90 m<sup>2</sup>/g should be attributed to more methylene blue molecules accessing to the expanded interflake space and the Al<sup>3+</sup> cations.

## CONCLUSIONS

We successfully synthesized a new family of nonflammable, water-stable, flexible, lightweight, and mechanically strong polymeric freestanding films of cl-GO, out of the highly flammable, fragile, and water-exfoliating GO. All experimental data consistently suggested the cl-GO to possess such a microstructure as illustrated in Figure 7.

This study confirmed the longstanding and so far not popularly known problem of the high flammability of the as-made GO from the modified Hummer's method and developed a facile route to solving the problem that can otherwise dangerously jeopardize the large-scale production and applications of the graphene-related materials. Moreover in materials chemistry, the cross-linking method should be generally applicable to polymerizing many types of layered 2D-materials (e.g., h-BN, MoS<sub>2</sub>, clays, etc.) and even nanocrystals, for meeting a new challenge in tailor-making advanced materials at low cost and high structural precision by design and on-demand.

## ASSOCIATED CONTENT

### Supporting Information

The Supporting Information is available free of charge on the ACS Publications website at DOI: 10.1021/acs.jpcc.6b13043.

Video from exposing to open flame with the GO (AVI)  
Video from exposing to open flame with the cl-GO (AVI)

## AUTHOR INFORMATION

### Corresponding Author

\*E-mail: rtian@uark.edu.

### ORCID

Z. Ryan Tian: 0000-0002-5644-8483

Wuzong Zhou: 0000-0001-9752-7076

### Notes

The authors declare no competing financial interest.

## ACKNOWLEDGMENTS

The authors acknowledge National Science Foundation-Experimental Program to Stimulate Competitive Research (NSF-EPSCoR) for partial support, Prof. S. Yu's lab for the micro-Raman experiments, and Dr. Jingyi Chen's lab for the TGA study.

## REFERENCES

- (1) Park, S.; Lee, K.-S.; Bozoklu, G.; Cai, W.; Nguyen, S. T.; Ruoff, R. S. Graphene Oxide Papers Modified by Divalent Ions-Enhancing Mechanical Properties via Chemical Cross-Linking. *ACS Nano* **2008**, *2*, 572–578.
- (2) Frank, I. W.; Tanenbaum, D. M.; van der Zande, A. M.; McEuen, P. L. Mechanical Properties of Suspended Graphene Sheets. *J. Vac. Sci. Technol. B Microelectron. Nanom. Struct.* **2007**, *25*, 2558.
- (3) Pacheco Sanjuan, A. A.; Wang, Z.; Imani, H. P.; Vanević, M.; Barraza-Lopez, S. Graphene's Morphology and Electronic Properties

from Discrete Differential Geometry. *Phys. Rev. B: Condens. Matter Mater. Phys.* **2014**, *89*, 121403.

(4) White, C. T.; Li, J.; Gunlycke, D.; Mintmire, J. W. Hidden One-Electron Interactions in Carbon Nanotubes Revealed in Graphene Nanostrips. *Nano Lett.* **2007**, *7*, 825–830.

(5) Pereira, J. M.; Vasilopoulos, P.; Peeters, F. M. Tunable Quantum Dots in Bilayer Graphene. *Nano Lett.* **2007**, *7*, 946–949.

(6) Zhang, Y.; Tan, Y.-W.; Stormer, H. L.; Kim, P. Experimental Observation of the Quantum Hall Effect and Berry's Phase in Graphene. *Nature* **2005**, *438*, 201–204.

(7) van den Brink, J. Graphene: From Strength to Strength. *Nat. Nanotechnol.* **2007**, *2*, 199–201.

(8) Park, S.; Ruoff, R. S. Chemical Methods for the Production of Graphenes. *Nat. Nanotechnol.* **2009**, *4*, 217–224.

(9) Kim, J.; Cote, L. J.; Kim, F.; Yuan, W.; Shull, K. R.; Huang, J. Graphene Oxide Sheets at Interfaces. *J. Am. Chem. Soc.* **2010**, *132*, 8180–8186.

(10) Marcano, D. C.; Kosynkin, D. V.; Berlin, J. M.; Sinitskii, A.; Sun, Z.; Slesarev, A.; Alemany, L. B.; Lu, W.; Tour, J. M. Improved Synthesis of Graphene Oxide. *ACS Nano* **2010**, *4*, 4806–4814.

(11) Huang, J.; Zhang, L.; Chen, B.; Ji, N.; Chen, F.; Zhang, Y.; Zhang, Z. Nanocomposites of Size-Controlled Gold Nanoparticles and Graphene Oxide: Formation and Applications in SERS and Catalysis. *Nanoscale* **2010**, *2*, 2733–2738.

(12) Xu, C.; Wang, X. Fabrication of Flexible Metal-Nanoparticle Films Using Graphene Oxide Sheets as Substrates. *Small* **2009**, *5*, 2212–2217.

(13) Pham, T. A.; Kim, J. S.; Kim, J. S.; Jeong, Y. T. One-Step Reduction of Graphene Oxide with L-Glutathione. *Colloids Surf., A* **2011**, *384*, 543–548.

(14) Janowska, I.; Chizari, K.; Ersen, O.; Zafeiratos, S.; Soubane, D.; Costa, V.; Da Speisser, V.; Boeglin, C.; Houllé, M.; Bégin, D.; et al. Microwave Synthesis of Large Few-Layer Graphene Sheets in Aqueous Solution of Ammonia. *Nano Res.* **2010**, *3*, 126–137.

(15) Kuila, T.; Mishra, A. K.; Khanra, P.; Kim, N. H.; Lee, J. H. Recent Advances in the Efficient Reduction of Graphene Oxide and Its Application as Energy Storage Electrode Materials. *Nanoscale* **2013**, *5*, 52–71.

(16) Mungse, H. P.; Verma, S.; Kumar, N.; Sain, B.; Khatri, O. P. Grafting of Oxo-Vanadium Schiff Base on Graphene Nanosheets and Its Catalytic Activity for the Oxidation of Alcohols. *J. Mater. Chem.* **2012**, *22*, 5427.

(17) Qiu, Y.; Collin, F.; Hurt, R. H.; Külaots, I. Thermochemistry and Kinetics of Graphite Oxide Exothermic Decomposition for Safety in Large-Scale Storage and Processing. *Carbon* **2016**, *96*, 20–28.

(18) Kim, F.; Luo, J.; Cruz-Silva, R.; Cote, L. J.; Sohn, K.; Huang, J. Self-Propagating Domino-like Reactions in Oxidized Graphite. *Adv. Funct. Mater.* **2010**, *20*, 2867–2873.

(19) Becerril, H. A.; Mao, J.; Liu, Z.; Stoltenberg, R. M.; Bao, Z.; Chen, Y. Evaluation of Solution-Processed Reduced Graphene Oxide Films as Transparent Conductors. *ACS Nano* **2008**, *2*, 463–470.

(20) Zhang, X.; Huang, Y.; Wang, Y.; Ma, Y.; Liu, Z.; Chen, Y. Synthesis and Characterization of a graphene–C60 Hybrid Material. *Carbon* **2009**, *47*, 334–337.

(21) Krishnan, D.; Kim, F.; Luo, J.; Cruz-Silva, R.; Cote, L. J.; Jang, H. D.; Huang, J. Energetic Graphene Oxide: Challenges and Opportunities. *Nano Today* **2012**, *7*, 137–152.

(22) Hummers, W. S.; Offeman, R. E. Preparation of Graphitic Oxide. *J. Am. Chem. Soc.* **1958**, *80*, 1339–1339.

(23) Lee, Y. R.; Kim, S. C.; Lee, H.; Jeong, H. M.; Raghu, A. V.; Reddy, K. R.; Kim, B. K. Graphite Oxides as Effective Fire Retardants of Epoxy Resin. *Macromol. Res.* **2011**, *19*, 66–71.

(24) Zhang, R.; Hu, Y.; Xu, J.; Fan, W.; Chen, Z.; Wang, Q. Preparation and Combustion Properties of Flame Retardant Styrene-Butyl Acrylate Copolymer/Graphite Oxide Nanocomposites. *Macromol. Mater. Eng.* **2004**, *289*, 355–359.

(25) Zhang, R.; Hu, Y.; Xu, J.; Fan, W.; Chen, Z. Flammability and Thermal Stability Studies of Styrene-butyl Acrylate Copolymer/

graphite Oxide Nanocomposite. *Polym. Degrad. Stab.* **2004**, *85*, 583–588.

(26) Higginbotham, A. L.; Lomeda, J. R.; Morgan, A. B.; Tour, J. M. Graphite Oxide Flame-Retardant Polymer Nanocomposites. *ACS Appl. Mater. Interfaces* **2009**, *1*, 2256–2261.

(27) Dasari, A.; Yu, Z.-Z.; Mai, Y.-W.; Cai, G.; Song, H. Roles of Graphite Oxide, Clay and POSS during the Combustion of Polyamide 6. *Polymer* **2009**, *50*, 1577–1587.

(28) Cui, W.; Guo, F.; Chen, J. Flame Retardancy and Toughening of High Impact Polystyrene. *Polym. Compos.* **2007**, *28*, 551–559.

(29) Bajaj, P. Fire-Retardant Materials. *Bull. Mater. Sci.* **1992**, *15*, 67–76.

(30) Dikin, D. A.; Stankovich, S.; Zimney, E. J.; Piner, R. D.; Dommett, G. H. B.; Evmenenko, G.; Nguyen, S. T.; Ruoff, R. S. Preparation and Characterization of Graphene Oxide Paper. *Nature* **2007**, *448*, 457–460.

(31) Li, D.; Kaner, R. B. Materials Science. Graphene-Based Materials. *Science* **2008**, *320*, 1170–1171.

(32) Loh, K. P.; Bao, Q.; Eda, G.; Chhowalla, M. Graphene Oxide as a Chemically Tunable Platform for Optical Applications. *Nat. Chem.* **2010**, *2*, 1015–1024.

(33) Eda, G.; Chhowalla, M. Chemically Derived Graphene Oxide: Towards Large-Area Thin-Film Electronics and Optoelectronics. *Adv. Mater.* **2010**, *22*, 2392–2415.

(34) Zhu, Y.; James, D. K.; Tour, J. M. New Routes to Graphene, Graphene Oxide and Their Related Applications. *Adv. Mater.* **2012**, *24*, 4924–4955.

(35) Kim, J.; Cote, L. J.; Huang, J. Two Dimensional Soft Material: New Faces of Graphene Oxide. *Acc. Chem. Res.* **2012**, *45*, 1356–1364.

(36) Hu, M.; Mi, B. Layer-by-Layer Assembly of Graphene Oxide Membranes via Electrostatic Interaction. *J. Membr. Sci.* **2014**, *469*, 80–87.

(37) Hung, W.-S.; Tsou, C.-H.; De Guzman, M.; An, Q.-F.; Liu, Y.-L.; Zhang, Y.-M.; Hu, C.-C.; Lee, K.-R.; Lai, J.-Y. Cross-Linking with Diamine Monomers To Prepare Composite Graphene Oxide-Framework Membranes with Varying D -Spacing. *Chem. Mater.* **2014**, *26*, 2983–2990.

(38) Hu, M.; Mi, B. Enabling Graphene Oxide Nanosheets as Water Separation Membranes. *Environ. Sci. Technol.* **2013**, *47*, 3715–3723.

(39) Han, Y.; Xu, Z.; Gao, C. Ultrathin Graphene Nanofiltration Membrane for Water Purification. *Adv. Funct. Mater.* **2013**, *23*, 3693–3700.

(40) Yeh, C.-N.; Raidongia, K.; Shao, J.; Yang, Q.-H.; Huang, J. On the Origin of the Stability of Graphene Oxide Membranes in Water. *Nat. Chem.* **2015**, *7*, 166–170.

(41) Tuinstra, F.; Koenig, J. L. Raman Spectrum of Graphite. *J. Chem. Phys.* **1970**, *53*, 1126–1130.

(42) Stankovich, S.; Dikin, D. A.; Piner, R. D.; Kohlhaas, K. A.; Kleinhammes, A.; Jia, Y.; Wu, Y.; Nguyen, S. T.; Ruoff, R. S. Synthesis of Graphene-Based Nanosheets via Chemical Reduction of Exfoliated Graphite Oxide. *Carbon* **2007**, *45*, 1558–1565.

(43) Fan, Z.; Wang, K.; Wei, T.; Yan, J.; Song, L.; Shao, B. An Environmentally Friendly and Efficient Route for the Reduction of Graphene Oxide by Aluminum Powder. *Carbon* **2010**, *48*, 1686–1689.

(44) Yang, D.; Velamakanni, A.; Bozoklu, G.; Park, S.; Stoller, M.; Piner, R. D.; Stankovich, S.; Jung, I.; Field, D. A.; Ventrice, C. A.; et al. Chemical Analysis of Graphene Oxide Films after Heat and Chemical Treatments by X-Ray Photoelectron and Micro-Raman Spectroscopy. *Carbon* **2009**, *47*, 145–152.

(45) Gómez-Navarro, C.; Weitz, R.; Bittner, A. M.; Scolari, M.; Mews, A.; Burghard, M.; Kern, K. Electronic Transport Properties of Individual Chemically Reduced Graphene Oxide Sheets. *Nano Lett.* **2007**, *7*, 3499.

(46) Eda, G.; Fanchini, G.; Chhowalla, M. Large-Area Ultrathin Films of Reduced Graphene Oxide as a Transparent and Flexible Electronic Material. *Nat. Nanotechnol.* **2008**, *3*, 270–274.

(47) Wang, X.; Jiao, L.; Sheng, K.; Li, C.; Dai, L.; Shi, G. Solution-Processable Graphene Nanomeshes with Controlled Pore Structures. *Sci. Rep.* **2013**, *3*, 1996.